

# MODELLING, PROTOTYPING AND TESTING NACRE-INSPIRED MICROSTRUCTURES FOR IMPROVED DAMAGE TOLERANCE

F. Narducci<sup>1</sup>, S. T. Pinho<sup>1</sup>

<sup>1</sup>Department of Aeronautics, Imperial College London

South Kensington Campus, London SW7 2AZ, United Kingdom

Email: f.narducci14@imperial.ac.uk, silvestre.pinho@imperial.ac.uk, Web Page: [tinyurl.com/pinholab](http://tinyurl.com/pinholab)

**Keywords:** Damage tolerance, biomimetics, strain hardening, nacre, microstructural design

## Abstract

In this work, a novel, bio-inspired carbon/epoxy composite with nacre-like tiled microstructure is designed and synthesised. Analytical models were developed to predict the strength and toughness of such composite, and the predictions for the stress-strain response during tile pull-out were validated against FE. Suitable configurations for tile geometry were then identified and used for the subsequent manufacturing, based on their capability to diffuse damage. The dimensions of the tiles as required for damage diffusion were found to be of the order of 0.7 mm. To prototype the material, two main challenges were overcome. The first was to cut accurate tiles of such small dimensions. The second was to successfully align the phase of tiles in one ply with that of neighbouring plies. The results show that both cutting and alignment were achieved with great accuracy. In-situ SEM testing is ongoing and will be presented at the conference.

## 1. Introduction

Carbon Fibre Reinforced Polymers (CFRPs) have been widely recognised as the material of choice for several automotive and aerospace applications, where a high strength-to-weight ratio is essential. However, the main limit to further extending the use of these materials is their low damage tolerance and damage diffusion capability, which often causes the composite structure to be oversized in order to avoid brittle failure.

Research on biological materials has recently proven that damage tolerance properties of composites stem from their design from the nano- and micro-structural level [1, 2]. From a biomimetics viewpoint, the toughening mechanisms that are commonly found in biological structures can in principle be extended to the design of synthetic composites with increased damage tolerance. In other words, control of the composite architecture at the microscale would allow us to reproduce features such as crack deflection, crack bridging and hierarchical failure [1, 3] that would help overcome the inherent brittleness of traditional man-made composites.

Among all biological composites, nacre, found in the inner layer of most seashells, provides one of the most striking trade-offs between strength and toughness. Nacre consists of a brick-and-mortar structure, in which hard aragonite tiles are embedded in a soft protein matrix (Figure 1). Despite being almost entirely made of a brittle ceramic phase, nacre is capable of large inelastic deformations (nearly 1% strain to failure [4]) and it has been proven to be up to 20-30 times tougher than monolithic aragonite (which makes up to 95% weight of the whole composite [5]). Hierarchical structure, tile pull-out, strain

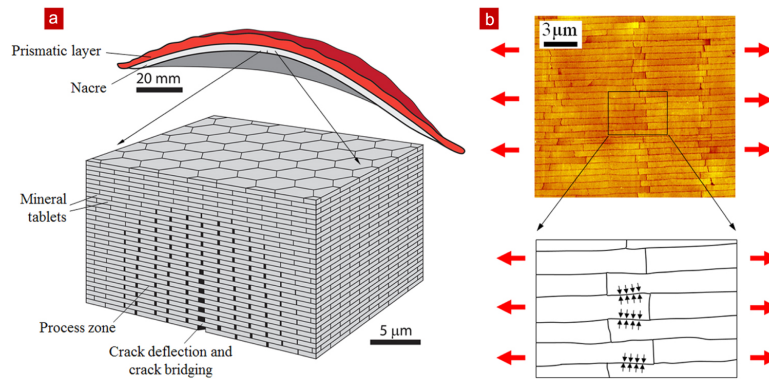


**Figure 1.** Microstructure of nacre (a) and detail of tile interlock (b) [7].

hardening [6] and damage diffusion [3] are among the reasons for this remarkable behaviour.

In this work, a CFRP composite with nacre-like microstructure is designed, prototyped and tested. The aim is to achieve higher levels of damage tolerance with respect to the carbon/epoxy parent material, and this will be done by designing the structure of the composite at the microscale. Several attempts have been made in the literature to design materials with nacre-inspired structure [5, 7], but few have directly addressed CFRPs for this purpose [8]. Furthermore, the emergence of thin-ply composite prepregs ( $\sim 20\ \mu\text{m}$  thick) allows us to now explore a larger design space, and the use of high-precision laser cutting technology has been demonstrated [9] to enable the imprinting of fine patterns in thin-ply.

## 2. Microstructure design

An artificial nacre-inspired composite is designed, in which each prepreg ply corresponds to an in-plane array of tiles that overlap by half of their length  $L$  (Figure 2). In order for our synthetic composite to reproduce a failure mechanism analogous to real nacre (where ceramic platelets do not break while being pulled apart, therefore dissipating a large amount of energy by friction [6]), tiles must remain intact during the pull-out process. Furthermore, the hardening required for damage diffusion is provided by the geometrical interlock of tiles [5, 10], which have an ‘hourglass’ shape in the  $x$ - $y$  plane, as shown in Figure 3. The shape and dimensions of tiles should be such that (a) tiles do not break during matrix debonding and subsequent pull-out, and (b) energy dissipated via friction during pull-out is maximised.

### 2.1. Shear-lag load transfer: optimal tile length

In order to calculate the stress profile on tiles, we assume that tiles carry tensile loads, whereas resin only undergoes shear; tensile loads are transferred from one tile to the other according to a shear-lag mechanism [11], as shown in Figure 4. The maximum load that tiles are subjected to corresponds to complete matrix debonding, after which they start sliding (pull-out). Because tiles are made of CFRP, their strength is size-dependent. Knowing the thickness  $t$  of the prepreg, the geometry of tiles is entirely defined by the following three parameters (see Figure 3):

- interlock angle  $\alpha$ ;
- in-plane aspect ratio  $\beta = \frac{H+h}{L}$ ;
- length  $L$ .

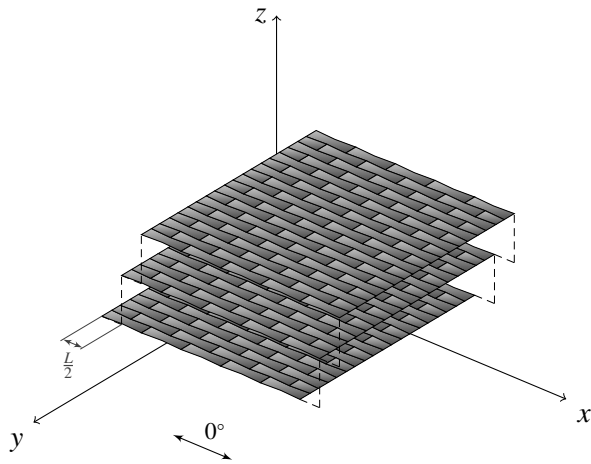


**Figure 2.** Tile arrangement of the nacre-inspired composite. Only three layers are shown for simplicity, with tiles overlapping by half of their length  $L$ .

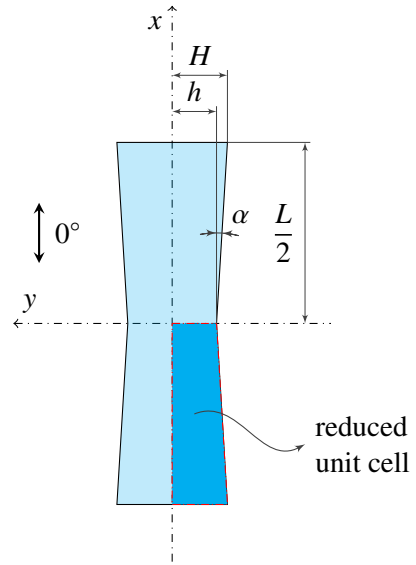


**Figure 3.** Geometry of tile and detail of the reduced unit cell used for the modelling. Fibres are all aligned in the longitudinal ( $x$ ) direction.

Therefore, given that a tile can be identified as a bundle of fibres, for a certain combination of  $\alpha$  and  $\beta$  we developed a model for tile stress distribution based on shear lag [12]. It is then possible to calculate the survival probability of the tile as a function of its length  $L$ , using the fibre bundle model derived from Pimenta and Pinho [13]. Because we want to ensure that tiles do not break (which implies short  $L$ ), but we want them to dissipate as much energy as possible by friction (which requires large  $L$ ), we will define as the length  $L_{99\%}(\alpha, \beta)$  the value corresponding to a tile survival probability of 99% (see Figure 5). This is the maximum value of length for which tiles can be assumed not to break, and is a function of  $\alpha$  and  $\beta$ .

## 2.2. Analytical model for tile interlock

After matrix debonding, tiles start sliding against each other under loading: if they are designed so as to not break (section 2.1), the pull-out length is  $L/2$ . Geometrical interlock is the mechanism that provides strain hardening during the pull-out process, forcing the remote stress to increase in order to slide tiles

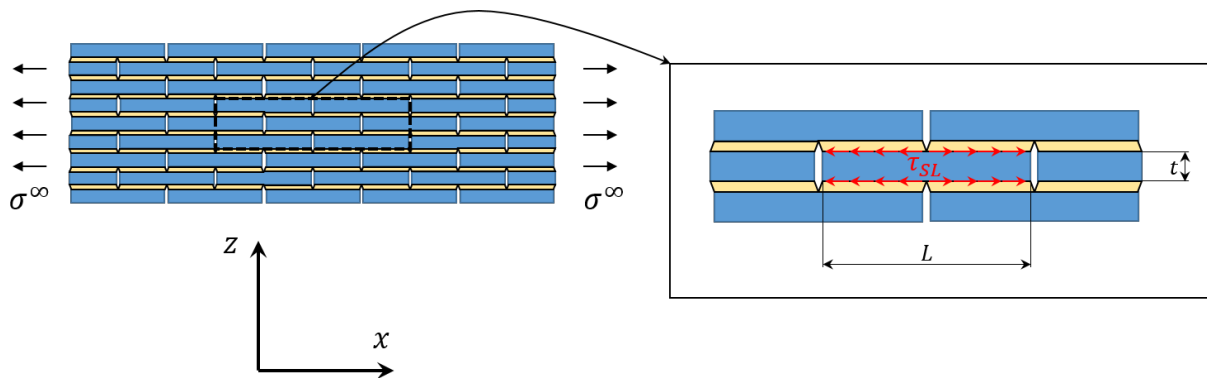


**Figure 4.** Through-the-thickness view of a tiled composite (left) and detail of shear-lag load transfer (right).

Excerpt from ISBN 978-3-00-053387-7

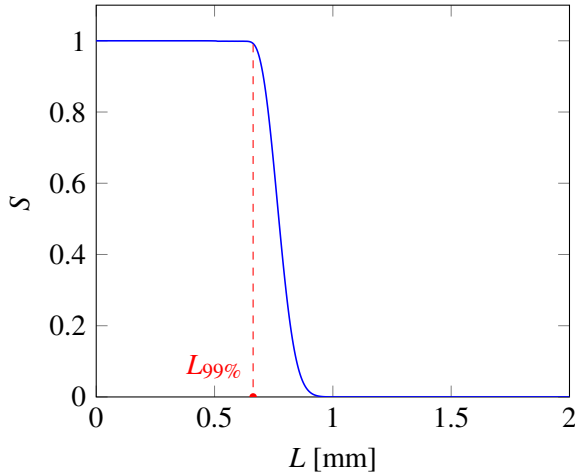


**Figure 5.** Survival probability  $S$  for a tile with  $\alpha = 3.5^\circ$  and  $\beta = 0.25$ , as a function of its length  $L$ . Material properties are derived from Cz el and Wisnom [13], assuming a shear-lag stress  $\tau_{SL} = 90$  MPa.

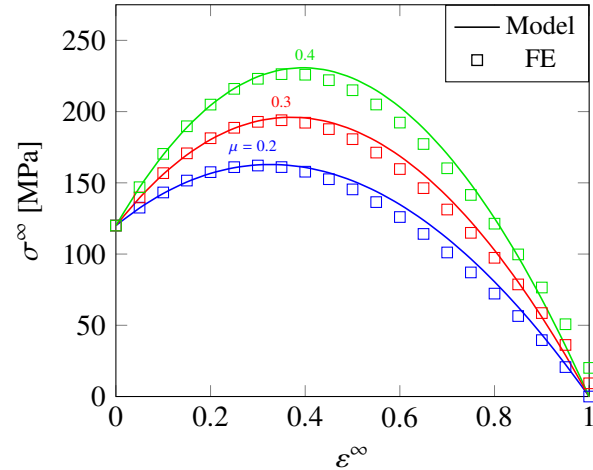


**Figure 6.** Analytical results for the pull-out stress-strain response of the unit cell and comparison with FE, for  $\mu = 0.2$  (blue),  $0.3$  (red) and  $0.4$  (green). Geometrical parameters are  $\alpha = 3.5^\circ$ ,  $\beta = 0.25$  and  $L = 0.66$  mm.

further. An analytical model has been developed [12] in order to predict the pull-out stress-strain response of the material, based on a ‘reduced’ unit cell (Figure 3), which is the smallest element representative of the whole structure, exploiting its symmetries. The remote stress  $\sigma^\infty$  required during pull-out can be calculated as a function of the longitudinal strain  $\varepsilon^\infty = u/b$ ,  $u$  being the pull-out displacement ( $u \in [0, L/2]$ ) and  $b = L/2$  being half the tile length:

$$\sigma^\infty = \frac{\sin \alpha + \mu \cos \alpha}{\cos \alpha - \mu \sin \alpha} E_y \frac{1 - \varepsilon^\infty}{2\beta} \frac{\tan \alpha \cdot \varepsilon^\infty}{2\beta + \tan \alpha \cdot \varepsilon^\infty} + \tau_\mu \frac{b}{t} (1 - \varepsilon^\infty), \quad (1)$$

where  $E_y$  is the transverse modulus of the tile material,  $\tau_\mu$  is the friction stress at the tile/tile interface during tile pull-out and  $\mu$  is the friction coefficient between tiles at the interlocking surface.

### 2.2.1. FE validation

The stress-strain response predicted by the model in Section 2.2 is validated against numerical results. A finite element model of the reduced unit cell (highlighted in Figure 3) is built using Abaqus 6.13, with a friction contact interaction between the two tiles in contact. Analytical and numerical predictions are compared in Figure 6 for different values of the friction coefficient  $\mu$ , showing good agreement.

### 2.2.2. Parametric study: optimal tile shape

Validation of the analytical model against FE allows us to use the former to run an efficient parametric study, in order to find the optimal geometrical configuration of tiles to use in the experiments. Knowing the elastic properties of the material and assuming a friction coefficient  $\mu = 0.3$ , the optimal tile shape will correspond to the combination of  $\alpha, \beta$  and  $L$  that maximises the energy (per unit volume) dissipated during tile pull-out, which corresponds to the area under the stress-strain curve of the unit cell (Figure 6), only calculated until the maximum hardening point (as damage localisation is expected upon softening of the material [6]).

For each combination of  $\alpha$  and  $\beta$ , the pull-out stress-strain relation is calculated (assuming a tile length  $L = L_{99\%}(\alpha, \beta)$  found as shown in section 2.1), providing the energy dissipated per unit volume. The

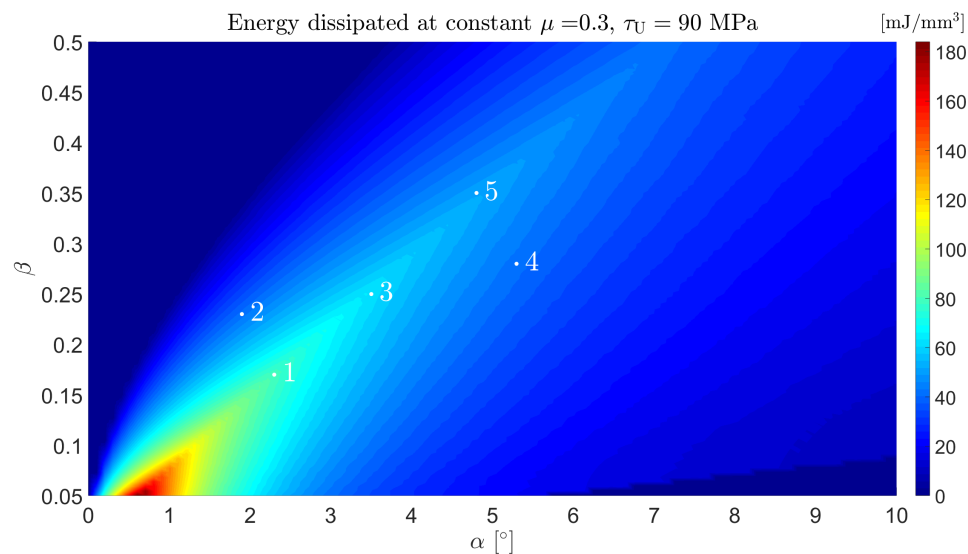


**Figure 7.** Map of the energy dissipated by the unit cell during tile pull-out until the maximum hardening point, as a function of  $\alpha$  and  $\beta$ . A friction coefficient  $\mu = 0.3$  and matrix ultimate strength  $\tau_U = 90$  MPa are assumed. The five geometrical configurations used in the experiments are highlighted.

results are shown in Figure 7, where the material considered is SkyFlex USN020A carbon/epoxy prepreg, which will be used in the experiments (material properties are derived from Czél and Wisnom [14]).

According to model predictions, the maximum energy is dissipated at very small values of  $\beta$ , which corresponds to extremely slender tiles. In theory, the energy would be infinite for  $\beta = 0$  (therefore null width,  $h = 0$  in Figure 3), but  $\beta \approx 0$  would correspond to having very few fibres in the tile cross-section, invalidating the assumption of homogenised material on which our models (both analytical and FE) rely.

### 3. Experimental

A nacre-like uni-directional composite was manufactured using SkyFlex USN020A carbon/epoxy prepreg. For the latter, a fibre volume fraction  $V_f = 42\%$  was measured by dissolving the uncured resin away in acetone and measuring the weight of the carbon fibre left. From Figure 7, five geometrical patterns for the tiles were selected (Table 1) considering the intention of maximising the energy dissipated, the manufacturing constraints, the interest in exploiting the design space, and the uncertainty in constituents and interface properties.

Tile patterns were engraved in the prepreg plies by laser cutting (using an Oxford Lasers DPSS Etcher) prior to layup and curing. This technique was found to provide the required level of accuracy and repeatability for the periodic pattern of tiles, as shown in Figure 8. A parametric study over the laser parameters (feed rate, power, number of passes) was performed in order to minimise the cut width  $w_{cut}$ , while still allowing removing the backing paper from the cut prepreg upon layup: power and number of passes need to be large enough to cut through the fibres, but small enough to avoid melting the resin onto the backing paper. As shown in Figure 8(f), for the chosen process parameters, the average  $w_{cut}$  is found to be around  $12 \mu\text{m}$ , the minimum and maximum measured values being  $10$  and  $15 \mu\text{m}$  respectively.

The layup of the UD structure was done by using alignment pins to provide the accurate positioning of each ply (61 plies in total). In order to achieve an efficient load transfer between tiles, these should overlap by half of their length  $L$  (see Figure 2), therefore it is essential to provide a precision of the

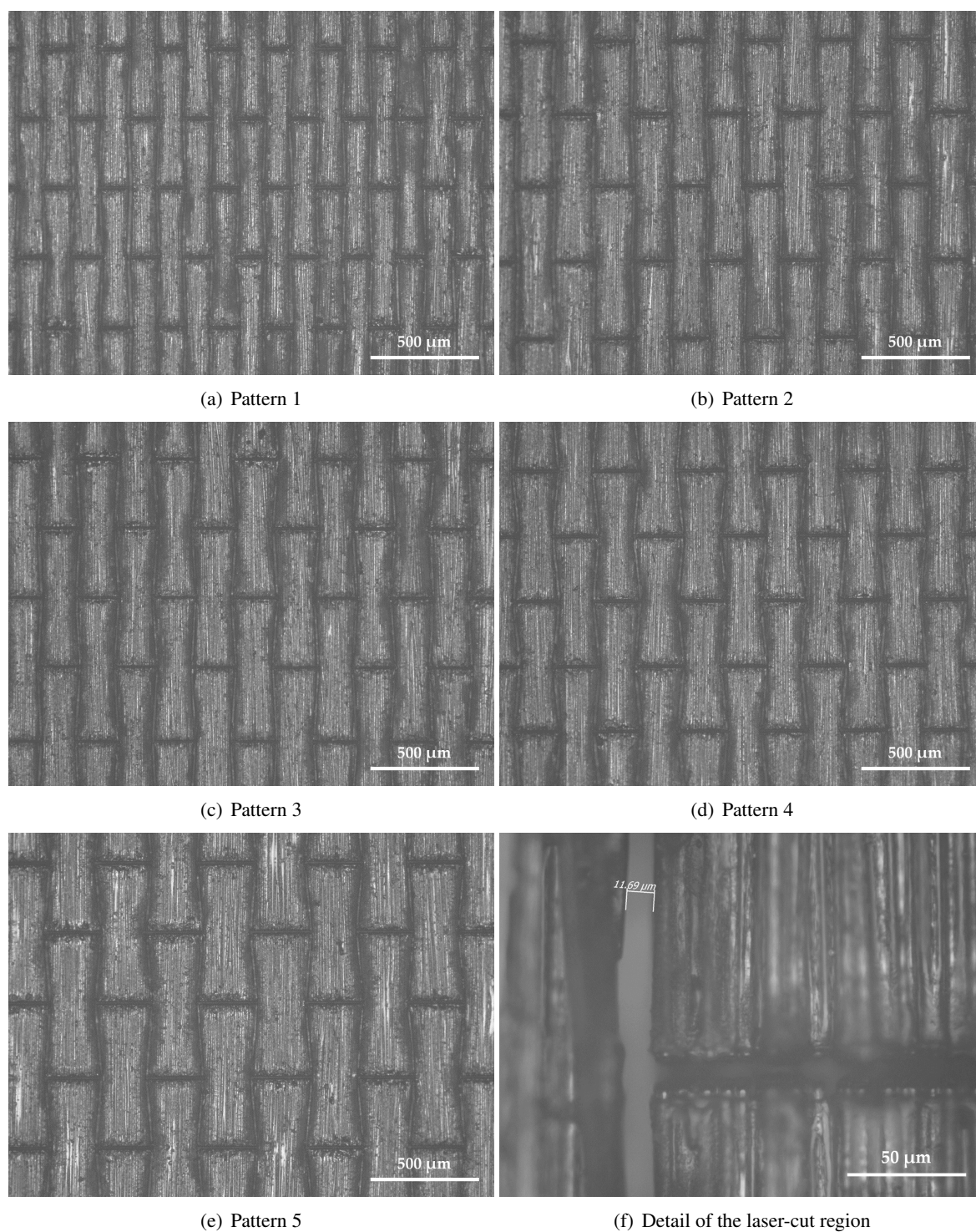


**Figure 8.** Optical images of the five patterns of tiles (a-e) and detail (f) of the average width of cut  $w_{cut}$  obtained by laser-cutting of the uncured prepreg

Excerpt from ISBN 978-3-00-053387-7

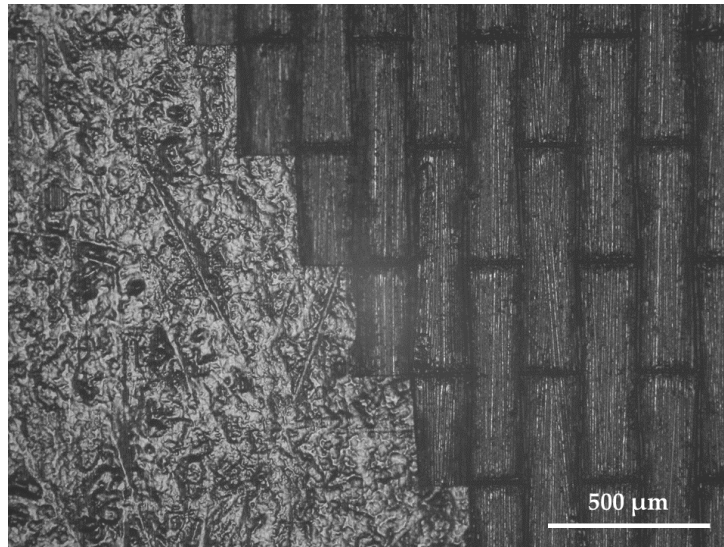


**Figure 9.** Example of the accuracy in the overlap of tiles, obtained by laying up two plies and then carefully removing some tiles from the top ply with a scalpel. The darker area on the right (with nacre pattern clearly visible) is the bottom ply, whereas the brighter region on the left is the top ply (cuts not clearly visible on the latter surface due to resin being squeezed into the gaps during vacuum-bagging).

order of the  $\mu\text{m}$  in the position of each ply. This challenge was successfully overcome by laser-cutting the alignment pinholes in the prepreg [9], thus keeping the same reference frame as the pattern of tiles. Figure 9 shows the level of precision that we can achieve in the relative positioning of plies with this technique.

**Table 1.** Geometrical parameters of the nacre-like specimens tested.

Pattern	Independent parameters			Dependent parameters	
	$\alpha$ [°]	$\beta$	$L$ [mm]	$h$ [ $\mu\text{m}$ ]	$H$ [ $\mu\text{m}$ ]
1	2.3	0.17	0.67	49.5	62.6
2	1.9	0.23	0.69	74.2	85.7
3	3.5	0.25	0.66	73.9	93.9
4	5.3	0.28	0.62	73.1	101.9
5	4.8	0.35	0.66	99.7	127.4

#### 4. Conclusions

A design solution for a CFRP composite with nacre-like microstructure was developed, allowing for the prototyping of a tiled structure in which the size of the unit cell is of the order of the millimeter. A laser-engraving technique was successfully developed and demonstrated to provide excellent accuracy and repeatability to the periodic pattern of tiles, and the latter were aligned with great precision despite the small scale of the structure. These bio-inspired composites will be tested in a three-point bending configuration in an SEM environment.

## Acknowledgments

Funding from EPSRC is hereby acknowledged, as well as Dr Steve Harrison at Triple H Composites Ltd for supplying the prepreg material used in this study.

## References

- [1] P-Y Chen, J McKittrick, and M A Meyers. Biological materials: functional adaptations and bioinspired designs. *Progress in Materials Science*, 57(8):1492–1704, 2012.
- [2] B Ji and H Gao. Mechanical principles of biological nanocomposites. *Annual Review of Materials Research*, 40:77–100, 2010.
- [3] F Barthelat and R Rabiei. Toughness amplification in natural composites. *Journal of the Mechanics and Physics of Solids*, 59(4):829–840, 2011.
- [4] F Barthelat and HD Espinosa. An experimental investigation of deformation and fracture of nacre–mother of pearl. *Experimental mechanics*, 47(3):311–324, 2007.
- [5] J Sun and B Bhushan. Hierarchical structure and mechanical properties of nacre: a review. *Rsc Advances*, 2(20):7617–7632, 2012.
- [6] R K Chintapalli, S Breton, A K Dastjerdi, and F Barthelat. Strain rate hardening: A hidden but critical mechanism for biological composites? *Acta biomaterialia*, 10(12):5064–5073, 2014.
- [7] S M M Valashani and F Barthelat. A laser-engraved glass duplicating the structure, mechanics and performance of natural nacre. *Bioinspiration & biomimetics*, 10(2):026005, 2015.
- [8] R Malkin et al. Bio-inspired laminate design exhibiting pseudo-ductile (graceful) failure during flexural loading. *Composites Part A: Applied Science and Manufacturing*, 54:107–116, 2013.
- [9] G Bullegas, S T Pinho, and S Pimenta. Bio-inspired microstructure design to improve translaminar fracture toughness of thin-ply composites. *International Conference on Composite Materials, Copenhagen, Denmark, 19-24 July 2015*.
- [10] AG Evans, Z Suo, RZ Wang, IA Aksay, MY He, and JW Hutchinson. Model for the robust mechanical behavior of nacre. *Journal of Materials Research*, 16(09):2475–2484, 2001.
- [11] S Pimenta and P Robinson. An analytical shear-lag model for composites with brick-and-mortar architecture considering non-linear matrix response and failure. *Composites Science and Technology*, 104:111–124, 2014.
- [12] F Narducci and S T Pinho. In preparation for publication. 2016.
- [13] S Pimenta and S T Pinho. Hierarchical scaling law for the strength of composite fibre bundles. *Journal of the Mechanics and Physics of Solids*, 61(6):1337–1356, 2013.
- [14] G Czél and MR Wisnom. Demonstration of pseudo-ductility in high performance glass/epoxy composites by hybridisation with thin-ply carbon prepreg. *Composites Part A: Applied Science and Manufacturing*, 52:23–30, 2013.